ISBN: 978-3-95450-231-8 ISSN: 2673-5490 doi: 10.18429/JACoW-IPAC2023-THPA047

OVERVIEW OF TOTAL IONIZING DOSE LEVELS IN THE LARGE HADRON COLLIDER DURING 2022 RESTART

Kacper Bilko*, R. Garcia Alia, Sylvain Girard, Marc Sebban
CERN, Geneva, Switzerland,
UJM, St-Etienne, France

Abstract

During the Large Hadron Collider (LHC) operation small fractions of the beam are lost continuously, leading to mixed-field radiation. Whereas the 2022 radiation environment in the majority of the locations follows expectations established both through measurements and simulations, some discrepancies with respect to the Run 2 operation (2015-2018) were detected. This work presents an overview of the 2022 Total Ionizing Dose (TID) levels as measured by the Beam Loss Monitors (BLMs) distributed along the LHC, focusing on the similarities and most prominent discrepancies in the arc sections with respect to the Run 2 operation.

INTRODUCTION

The Large Hadron Collider (LHC) is a circular machine at the European Organization for Nuclear Research (CERN) that collides two particle beams in the centres of four large experiments (ATLAS, CMS, LHCb and ALICE) [1]. During its operation, there are beam losses that generate mixed-field radiation in the proximity of the accelerator. This radiation can affect nearby electronic equipment by causing Single Event Effects (SEEs), displacement damages, and Total Ionising Dose (TID) effects. As a result, equipment failures could halt the operation of the LHC, reducing its overall performance [2].

LHC layout

The four experiments at the LHC are located in the four Long Straight Sections (LSSs), while the other four LSSs contain accelerator systems such as collimators (LSS3 and LSS7), radio-frequency cavities (LSS4), and the beam dumps (LSS6). The LSSs are surrounded by Dispersion Suppressor (DS) sections, which together form the Insertion Regions (IRs). The arc sections contain periodic arrangements (constituting a FODO lattice) of magnets that bend and focus the beam. A cell in the LHC arcs consists of a focusing quadrupole magnet, three bending dipole magnets, a defocusing quadrupole, and another three bending magnets.

The LHC is organized into small subsections called half-cells. Each arc section begins in the 12th half-cell of an IR and ends in the 12th half-cell of the next IR. For example, arc 45 extends between the right of IR4 and the left of IR5. Each arc half-cell contains a main quadrupole and three main bending dipoles.

LHC operation

The LHC is operated in a sequence of fills. Typical LHC fill contains several beam injections delivered by the Super Proton Synchrotron [3]. After the accomplished injection phase, the beams are accelerated from 450 GeV to 6.8 TeV. After reaching the top energy and adjusting the accelerator parameters, the beams are collided at the four aforementioned experimental Interaction Points (IPs). The main intensity statistics are listed in Tab. 1. Neglecting the pilot operation in 2021 (two weeks), 2022 was the first full year after the Long Shutdown 2 (LS2, 2019-2021). Integrated beam intensity (ATLAS/CMS luminosity) in 2022 corresponded to 58% (63%) of what was integrated in 2018, therefore the absolute 2022 TID levels are expected to be ≈ 60% of 2018's TID.

Table 1: Injected and time-integrated beam intensities as measured in 2022 and in the years of Run 2 (2015-2018) [4].

	Injected protons	Protons lost due to luminosity burn-off	Protons lost elsewhere	Time-integrated beams intensity	Time of beam-in
unit	10^{16} p	%	%	10^{19} ps	days
2022	13.5	48	52	179	101.2
2018	15.0	55	45	306	140.5
2017	13.8	59	41	251	124.8
2016	9.6	72	28	260	138.7
2015	5.6	26	74	72	109.6

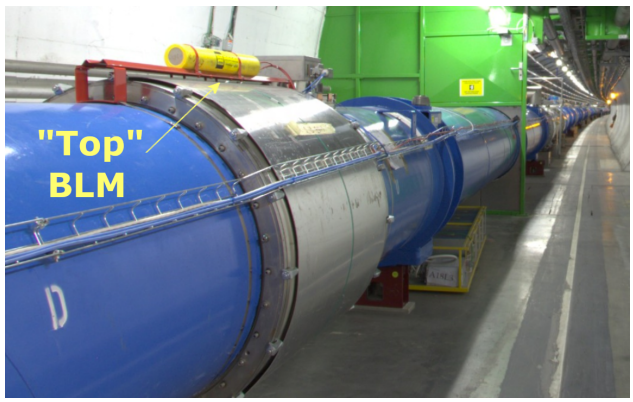

Figure 1: BLM installed in an LHC arc sector on top of the interconnection between the LHC dipole magnets. Each arc half-period contains 2 BLMs installed on top of the dipole interconnects, and 4 BLMs in the vicinity of the LHC quadrupole magnets.

* kacper.bilko@cern.ch

ISBN: 978-3-95450-231-8 ISSN: 2673-5490 doi: 10.18429/JACoW-IPAC2023-THPA047

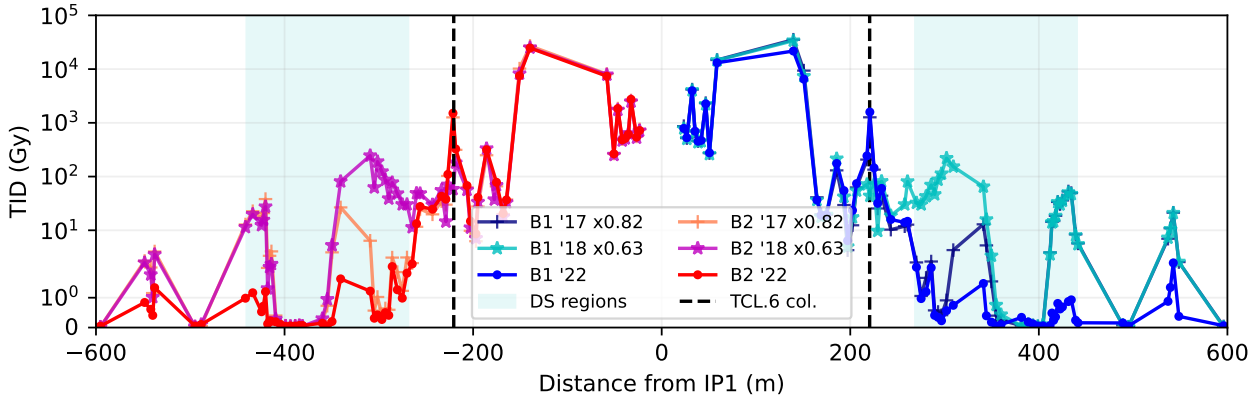

Figure 2: TID measured by the BLMs around ATLAS experiment in 2022, 2018, and 2017. B1 (B2) trace corresponds to monitors installed at the side of Beam 1 (2). Measurements in 2018 and 2017 were multiplied by the factors corresponding to the ratio of the integrated ATLAS luminosity with respect to 2022.

LHC Radiation Monitoring

CERN developed the beam loss monitoring system to safeguard the accelerator components and prevent superconducting magnet quenches. The system is composed of over 3600 Beam Loss Monitors (BLMs) [5], which are ionisation chambers filled with nitrogen gas and situated at critical locations around the LHC. An example of BLM is depicted in Fig. 1. Although the system's primary function is not dosimetry, through the dedicated data processing [6], this system can be exploited for TID measurements [7–9]. Within this work, we focus primarily on the arc sections, where the installation pattern of the BLMs reflects the periodic magnet arrangement, and each ARC half-cell contains 6 BLMs at different locations which are periodically repeated. This was previously described in detail [10].

TID LEVELS IN INSERTION REGIONS

TID levels in 2022 at IR1 and IR5 measured within $\pm$200 m were similar to Run 2, taking into account the respective integrated luminosity. The main differences were observed in their DS regions, i.e. ATLAS and CMS. As depicted in Fig. 2 for IR1, due to the smaller aperture of the TCL6 collimators, the radiation levels were locally higher (factor ~ 40). However, due to the more efficient beam cleaning, the radiation levels in the DS regions were lowered by more than 2 orders of magnitude. Similar observations were found for IR5. Other TID increases were found in IR4, particularly in the 6$^{\text{th}}$ and 7$^{\text{th}}$ half-cells of the right side of Point 4 where the TID normalized with the time-integrated beam intensity were factor 13 larger in 2022, as compared with 2018.

RADIATION IN THE LHC ARCS

In the majority of locations along the LHC arc sectors, the losses are expected to be driven by the interaction of a beam with the residual gas molecules in the vacuum chamber [10]. For a given energy (thus a given inelastic interaction cross-section σ), the related typical (*baseline*) dose rates ($\dot{D}$) are therefore proportional to the beam intensity (N) and the residual gas density (ρ), as expressed in (1). The proportionality is through the LHC beam revolution frequency f and the length of interaction regions (d).

$$\dot{D} = -\sigma d \rho f N(t) \tag{1}$$

However, it was observed that in several locations the radiation levels significantly exceeded the baseline [11]. In these locations interactions of the beams with residual gas molecules are no longer the dominating beam loss mechanism and the related TID levels are significantly higher.

Typical TID levels

For this study, we subselected BLMs installed on top of the interconnectors between main dipole magnets (Fig. 1), as these are less prone to the luminosity-driven beam losses, as compared to the side BLMs installed at the quadrupole magnets, where the $\beta_{x,y}$ functions reach its extreme values, and therefore the physical beam size is the largest. It was observed that the intensity-normalized baseline radiation levels decrease over time, both in the long term (elapsed time since the last shutdown) and in the short term, within each fill. Assuming beam-residual gas interactions are the dominating beam loss mechanism, the variations in the averaged normalized dose rate implicate the change of the residual gas density, following the equation $\rho \propto \frac{\dot{D}}{N_{12}}$, e.g. due to synchrotron radiation [12].

Intra-fill analysis As depicted in Fig. 3, the intensity-normalized baseline TID levels decrease in each LHC fill. The baseline dose rate was calculated as a mean value of the middle 50% of dose rates measured by Top BLMs in each arc sector. Provided that the dominating beam loss mechanism is the interaction of a beam with residual gas, this variability implies that the gas density encountered by the beam decreases during the beam circulation. Moreover,

ISBN: 978-3-95450-231-8 ISSN: 2673-5490 doi: 10.18429/JACoW-IPAC2023-THPA047

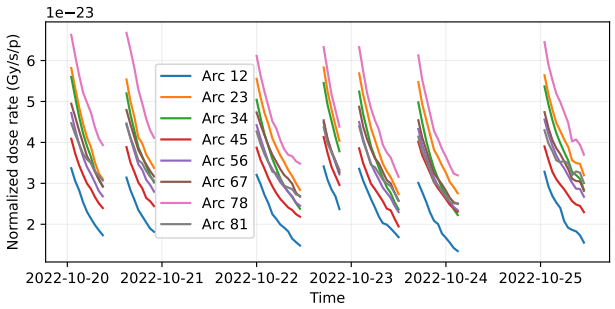

Figure 3: Baseline dose rate during physics production (beam collisions), normalized with the beam intensity, as a function of time for several LHC fills in 2022.

it partially recovers after the beam is extracted from the accelerator.

Long-term evolution In addition to the variability within a fill, it was observed, that there is an additional, long-term trend that involves a gradual decrease in the normalized dose rate and lower variability within a fill. This behaviour, for arc 34 as an example, is depicted in Fig. 4. One of the explanations would be reaching the conditioned vacuum state in which further vacuum improvement is no longer observable and the normalized dose rate constant. This (approximately) could be observed for fills depicted with green colour, corresponding to years 2017 and 2018.

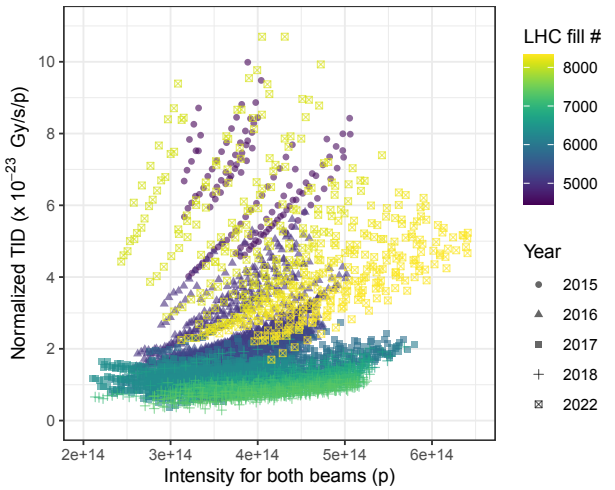

Figure 4: Normalized baseline dose rate (as calculated by the top BLMs) in Arc 34 of the LHC as a function of the intensity for both beams. Each point corresponds to the 1 h averaged value during physics collisions. The considered fills span between 2015 and 2022.

Variability among sectors The reported residual gas dynamics, both within a single fill and over multiple fills, was observed in all arc sectors, with varying magnitude. As depicted in Fig. 5, in 2022 the lowest baseline radiation levels were measured in arc 12, as opposed to Run 2, when these levels were the highest. In 2022, the worst conditioning (largest baseline TIDs) was observed in arcs 23 and 78.

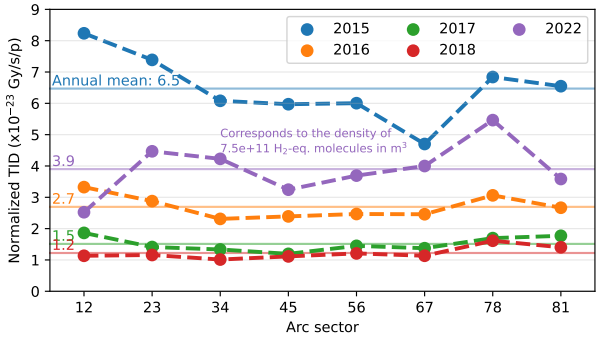

Figure 5: Annual baseline TID levels per arc sectors normalized with the total integrated intensity (for both beams).

Space-localised radiation peaks

In several locations of the arc sectors, the losses were driven by the luminosity-driven loss mechanisms, i.e. occurred only once the beams were collided.

Focusing on the most prominent peaks (with annual 2022 TID in a half-cell exceeding 1 Gy), 13 half-cells were identified. The largest 2022 arc TID value corresponded to 17 Gy (13R5, 13th half-cell of the Right side of Point 5). Among those, the majority were caused by the CMS (19R4, 15L5, 13L5, 13R5, 23R5, 19L6) and ATLAS (19R8, 13R1, 19L2) luminosity production. However, there are some half-cells (13R7, 18R7, 16L8, 16R2) with a not well-understood origins, that are under investigation.

CONCLUSIONS

Within this work, we presented the main intensity statistics and TID levels along the LHC, as measured by the BLMs in 2022. The main focus was on the LHC arc sectors, consisting of more than 70% of LHC circumference, and hosting multiple electronic systems (Quench Protection System, Power Converters), that could suffer from radiation effects on electronics [13].

Despite the 2022 baseline TID levels being higher 3 times with respect to 2018, it was found, that, similarly to the 2015 recommissioning, there is a dynamic improvement of the vacuum quality along the operation. Additionally, it was shown that the intensity normalized baseline dose rates decrease within each fill, implying a dynamic change in the residual gas density.

As already reported in Run 2 there are several localized radiation peaks that significantly exceed the baseline levels, in most cases caused by the collision in the experiments.

Concerning the other regions of the LHC, the most R2E-relevant changes were observed in the DS regions of IR1 and IR5 where, due to the tighter aperture of TCL6 collimators, the TID levels were reduced by more than 2 orders of magnitude.

ISBN: 978-3-95450-231-8 ISSN: 2673-5490 doi: 10.18429/JACoW-IPAC2023-THPA047

REFERENCES

[1] L. Evans and P. Bryant, "LHC machine," J. Inst., vol. 3, no. 8, Aug. 2008, Art. no. S08001.

[2] Y.Q. Aguiar et al., "Radiation to Electronics Impact on CERN LHC Operation: Run 2 Overview and HL-LHC Outlook", in Proc. IPAC'21, Campinas, SP, Brazil, May 2021, pp. 80-83. doi:10.18429/JACoW-IPAC2021-MOPAB013

[3] K. Biłko et al., "CERN Super Proton Synchrotron radiation environment and related Radiation Hardness Assurance implications," in IEEE Transactions on Nuclear Science, doi: 10.1109/TNS.2023.3261181.

[4] K. Bilko, O. Stein, "Report on the Prompt Dose Distribution Along the LHC Based on BLM Data for proton-proton operation in Run 2", CERN, Geneva, Switzerland, Rep. CERN-ACC-NOTE-2019-0040, Oct. 2019.

[5] B. Dehning et al., "LHC beam loss detector design: Simulation and measurements," in Proc. IEEE Part. Accel. Conf. (PAC), Jun. 2007, pp. 4198–4200.

[6] K. Biłko, R. García Alía, and J.B. Potoine, "Automated Analysis of the Prompt Radiation Levels in the CERN Accelerator Complex", in Proc. IPAC'22, Bangkok, Thailand, Jun. 2022, pp. 736-739. doi:10.18429/JACoW-IPAC2022-MOPOMS043

[7] O. Stein et al., "A Systematic Analysis of the Prompt Dose Distribution at the Large Hadron Collider", in Proc. 9th Int. Particle Accelerator Conf. (IPAC'18), Vancouver, BC, Canada, Apr. 4, pp. 2036-2038, doi:10.18429/JACoW-IPAC2018-WEPAF082

[8] O. Stein et al., "Run 2 Prompt Dose Distribution and Evolution at the Large Hadron Collider and Implications for Future Accelerator Operation", in Proc. IPAC'19, Melbourne, Australia, May 2019, pp. 4013-4015. doi:10.18429/JACoW-IPAC2019-THPRB084

[9] D. Prelipcean et al., "Comparison Between Run 2 TID Measurements and FLUKA Simulations in the CERN LHC Tunnel of the Atlas Insertion Region", in Proc. IPAC'22, Bangkok, Thailand, Jun. 2022, pp. 732-735. doi:10.18429/JACoW-IPAC2022-MOPOMS042

[10] K. Biłko et al., "Radiation Environment in the LHC Arc Sections During Run 2 and Future HL-LHC Operations," in IEEE Transactions on Nuclear Science, vol. 67, no. 7, pp. 1682-1690, July 2020, doi: 10.1109/TNS.2020.2970168.

[11] K. Bilko et al., "Detailed Analysis Of The Baseline Dose Levels And Localized Radiation Spikes In The Arc Sections Of The Large Hadron Collider During Run 2", in Proc. IPAC'19, Melbourne, Australia, May 2019, pp. 4009-4012. doi:10.18429/JACoW-IPAC2019-THPRB083

[12] V. Baglin et al., "Synchrotron Radiation in the LHC Vacuum System", in Proc. IPAC'11, San Sebastian, Spain, Sep. 2011, pp. 1563-1565.

[13] R. García Alía et al., "LHC and HL-LHC: Present and Future Radiation Environment in the High-Luminosity Collision Points and RHA Implications" in IEEE Transactions on Nuclear Science, vol. 65, no. 1, pp. 448-456, Jan. 2018, doi: 10.1109/TNS.2017.2776107.